Echinacoside ameliorates doxorubicin-induced cardiac injury by regulating GPX4 inhibition-induced ferroptosis

YAN MA, XIAOLI YANG, NIANXIN JIANG, CHENG LU, JIEHAN ZHANG and SHAOWEI ZHUANG

Department of Cardiology, Seventh People's Hospital of Shanghai University of Traditional Chinese Medicine, Shanghai 200137, P.R. China

Received April 20, 2023; Accepted August 15, 2023

DOI: 10.3892/etm.2023.12317

Abstract. Echinacoside (ECH) is a compound derived from the natural herbs *Cistanche* and *Echinacea*, which has considerable protective effects on heart failure (HF). HF is characterized by myocardial damage and abnormal ferroptosis. Glutathione peroxidase 4 (GPX4) is an important regulator of ferroptosis, which plays a role in ferroptosis-related diseases. Despite this, the therapeutic mechanisms of ECH against HF remain unknown. Therefore, the aim of the present study was to investigate the cardioprotective effect and underlying mechanisms of ECH in the treatment of doxorubicin (DOX)-induced chronic HF (CHF). Cell proliferation was assessed using a CCK-8 assay. Furthermore, cardiac cell injury and oxidative stress were determined by measuring the lactate dehydrogenase (LDH), malondialdehyde (MDA), and glutathione (GSH) levels. The levels of Fe^{2+} and lipid reactive oxygen species (ROS), and expression of the biomarkers of ferroptosis, including GPX4 and prostaglandin-endoperoxide synthase 2 (PTGS2), were measured to examine cardiomyocyte ferroptosis. Additionally, RNA interference was used to silence *Gpx4*. *In vitro* and *in vivo*, ECH considerably reduced the MDA and LDH levels and increased the GSH level, thereby attenuating DOX-induced cardiac injury and oxidative stress. Meanwhile, ECH treatment decreased the lipid ROS levels and PTGS2 expression while increasing GPX4 expression, thereby alleviating DOX-induced cardiomyocyte ferroptosis. Moreover, knockdown of *Gpx4* inhibited the protective effects of ECH on DOX-induced accumulation of lipid ROS in cardiomyocytes. These findings indicate that ECH can reduce DOX-induced cardiac injury by inhibiting ferroptosis via GPX4, highlighting its value as a potentially valuable therapeutic target in the management of CHF.

Correspondence to: Dr Jiehan Zhang or Dr Shaowei Zhuang, Department of Cardiology, Seventh People's Hospital of Shanghai University of Traditional Chinese Medicine, 358 Datong Road, Gaoqiao Town, Pudong New Area, Shanghai 200137, P.R. China
E-mail: jiehanzhang@163.com
E-mail: zhuangs_tcm@163.com

Key words: echinacoside, chronic heart failure, ferroptosis, glutathione peroxidase 4

Introduction

Heart failure (HF) is now one of the most common causes of cardiovascular disease, with increasing morbidity and mortality rates (1), and HF occurrence is closely related to the long-term survival of patients with acute coronary syndrome (2). Chronic HF (CHF) is a common complication of several heart diseases, characterized by impaired ventricular filling and ejection (3). Diabetes, hypertension, coronary heart disease, and chronic renal diseases are all risk factors for CHF (4). Doxorubicin (DOX) is an anthracycline initially extracted and identified from *Streptomyces pneumonia* (5). The highly effective anticancer drug DOX causes progressive cardiac remodeling due to myocardial damage during the early stages of treatment and leads to cardiomyopathy in the later periods (6), involving the excessive generation of reactive oxygen species (ROS), mitochondrial dysfunction, and cardiomyocyte death, frequently resulting in hospitalization (7,8). Additionally, cardiac cell injury, left ventricular dysfunction, and congestive HF associated with a high dose of DOX treatment further worsen a patient's quality of life (9). DOX-induced cardiotoxicity is a side effect when used to treat CHF.

Ferroptosis is a relatively newly discovered type of programmed cell death characterized by iron overload-induced production of large amounts of ROS and lipid peroxide flocking (10). Excessive death of myocardial cells can lead to various cardiovascular diseases and even develop into HF, so developing ideal treatment plans based on pathogenesis is of great significance for cardiopathy (11). Cardiac remodeling is widely accepted as the primary mechanism underlying the progression of HF (12). Cardiac remodeling causes myocardial fibrosis and hypertrophy, resulting in cardiac size, shape, and functional changes, eventually leading to cardiac systolic or diastolic dysfunction (13). Current studies have found that the mechanisms related to ferroptosis, including iron homeostasis imbalance, GSH deficiency, oxidative stress, cardiac stimulation, and mitochondrial dysfunction, play a role in cardiac remodeling (14). Substantial evidence has shown a close relationship between HF pathogenesis and the mechanism of ferroptosis, as the mechanism of HF and ferroptosis has been studied (15). Iron homeostasis is a complex process

regulated by multiple iron metabolism proteins; iron homeostasis imbalances can lead to iron overload and ferroptosis. Iron homeostasis plays an important role in maintaining normal heart physiological function, which is susceptible to iron overload, resulting in oxidative stress, and promoting the development of HF (16). Furthermore, the activation center of GPX4 is an important component of cysteine and prevents ferroptosis caused by lipid ROS, implying that GPX4-related ferroptosis may be important in CHF.

Echinacoside (ECH) is a natural bioactive compound isolated from the natural herbs *Cistanche* and *Echinacea*. ECH has several biological and pharmacological activities, including anti-apoptotic, neuroprotective, hepatoprotective, immunomodulatory, anti-aging, anti-diabetic, and bone formation-promoting properties (17,18). However, there are no studies assessing the cardioprotective effects of ECH in CHF to the best of our knowledge, and the potential underlying mechanisms remain elusive. Thus, the aim of the present study was to investigate the effects of ECH in GPX4 inhibition-induced ferroptosis of cardiomyocytes *in vivo* and *in vitro*.

Materials and methods

Cell culture and treatment. Rat H9c2 cells were obtained from The Cell Bank of Type Culture Collection of The Chinese Academy of Sciences. Cells were cultured in DMEM supplemented with 10% FBS, 2 mM l-glutamine, and 1% penicillin/streptomycin (all from Thermo Fisher Scientific, Inc.) at 37˚C in a humidified incubator supplied with 5% CO_2 air. DOX (2 μM, MilliporeSigma, cat. no. 25316-40-9) was used to create the model of using H9c2 cells pretreated for 24 h with or without 5, 10, or 20 μM ECH (purity: ≥99.85%; MedChemExpress, cat. no. HY-N0020). Otherwise, 35 μM erastin was used to induce ferroptosis in H9c2 cells pretreated for 24 h with or without 10 μM ECH.

CCK-8 assay. The CCK-8 assay (Signalway Antibody LLC) was used to detect cell proliferation. Cells were incubated with CCK-8 solution for 1 h after 0 and 24 h in culture. Cell proliferation was measured using a microplate reader, and optical densities at 450 nm were assessed. Each experiment was repeated three times.

Knockdown of Gpx4. Short hairpin-interfering RNAs (shRNA) targeting rat *Gpx4* (shGpx4-1: 5'-GGTTTGACATGT ACAGCAA-3', site: 377-398; shGpx4-2, 5'-GAAGTAATC AAGAAATCAA-3', site: 332-353; and shGpx4-3 5'-GGATGA AAGTCCAGCCCAA-3', site: 437-458) and scramble shRNA (5'-GGACGAGCTGTACAAGTAA-3') were produced by General Bio Co., Ltd. and assembled into lentiviral plasmids (pLKO.1). Recombinant plasmids were expressed in 293T cells in the presence of psPAX2 and pMD2G using Lipofectamine® 2000 (Thermo Fisher Scientific, Inc.) as per the manufacturer's instructions to produce transducer plasmids. After 48 h, cells were transduced with the pLKO.1-scramble shRNA (shNC) as a negative control.

Measurement of biochemical indices. The Fe^{2+} concentration in H9c2 cells was determined using an Iron Assay kit (cat. no. ab83366, Abcam), and the LDH (cat. no. A020-1-1), GSH (cat. no. A006-2-1), and MDA levels (cat. no. A003-1-1) in H9c2 cells or serum samples were determined using commercial biochemical kits (Jiancheng Bioengineering Institute). All procedures were performed in accordance with the manufacturer's protocols.

Lipid peroxidation assessment using C11-BODIPY. A total of 10 μM C11-BODIPY (Thermo Fisher Scientific, Inc.) was added to the cell suspension ($1x10^6$ cells/ml), and the suspension was incubated in the dark at 37˚C for 30 min. Cells were then washed with PBS, and the fluorescence intensity of the dye C11-BODIPY was measured using an Accuri™ C6 flow cytometer (BD Biosciences, Inc.). Data were analyzed using FlowJo version 7.6.1 (FlowJo LLC).

Reverse transcription-quantitative (RTq)PCR. Total RNA of different samples was extracted using TRIzol® Reagent (Invitrogen; Thermo Fisher Scientific, Inc.). Using a cDNA synthesis kit, RNA was reverse-transcribed into cDNA using a PrimeScript™ kit (Takara Biotechnology Co., Ltd.) according to the manufacturer's protocol. For qPCR, the thermocycling conditions were: 95˚C for 10 min; followed by 40 cycles of 95˚C for 15 sec and 60˚C for 45 sec, and *Gapdh* was used as the loading control. The relative gene expression was calculated using the $2^{-\Delta\Delta Cq}$ method (19). Data are presented as the mean of three replicates. Table I contains the sequences of all the primers.

Western blot analysis. RIPA lysis buffer (JRDUN) was used to lyse the samples, and the protein yield was determined using an enhanced BCA protein assay kit (Thermo Fisher Scientific, Inc.). Total proteins were separated by 10% SDS-PAGE and transferred to a nitrocellulose membrane overnight before being blocked with 5% nonfat dry milk overnight at 4˚C. Subsequently, membranes were incubated with one of the primary antibodies overnight at 4˚C, followed by secondary antibody anti-mouse IgG (cat. no. A0208; Beyotime Institute of Biotechnology; 1:1,000) for 1 h at 37˚C. Signals were visualized and densitometry analysis was performed using an enhanced chemiluminescence system (Bio-Rad Laboratories, Inc.). The primary antibodies were used: GPX4 (cat. no. DF6701; Affinity Biosciences Ltd.; 1:1,000), PTGS2 (cat. no. AF7003; Affinity Biosciences Ltd.; 1:1,000), and GAPDH (cat. no. #5174s; Cell Signaling Technology, Inc.; 1:30,000).

Rat model of CHF and treatments. Male Sprague-Dawley rats weighing 180-220 g were purchased from HFK Bioscience Co. Ltd. All experimental procedures were performed in accordance with the Guidelines for the Institutional Animal Care and Use Committee of Shanghai Rat & Mouse Biotech Co., Ltd. (Approval no. 202109) (18). All procedures followed internationally recognized ethical standards. The rats were divided into the following four groups (n=6 per group): normal group, DOX group (rat model of CHF), DOX + E50 group (DOX + ECH 50 mg/kg), and DOX + E100 group (DOX + ECH 100 mg/kg). A CHF rat model was induced by DOX (intraperitoneal injection of 2.5 mg/kg, twice a week) as previously described (7). Furthermore, the rats were given ECH (50 or 100 mg/kg) by gavage for 2 weeks. To monitor cardiac function, an echocardiogram was performed, and hemodynamic variables were

Table I. Sequences of the primers.

Gene	Forward	Reverse
Tfrc	5'-GTTTCTGCCAGCCCCCTATT-3'	5'-CACCTCTGCTGCTGTACGAA-3'
Slc11a2	5'-TCCCCATTCCTGAGGAGGAG-3'	5'-ATCCGTGGGACCTTGGGATA-3'
Slc7a11	5'-TCGTCCTTTCAAGGTGCCTC-3'	5'-AGAGTCTTCTGGTACAACTTCTAGT-3'
Gpx4	5'-ACGCCAAAGTCCTAGGAAGC-3'	5'-CTGCGAATTCGTGCATGGAG-3'
*Ptgs*2	5'-CTCAGCCATGCAGCAAATCC-3'	5'-GGGTGGGCTTCAGCAGTAAT-3'
Gapdh	5'-GGAGTCTACTGGCGTCTTCAC-3'	5'-ATGAGCCCTTCCACGATGC-3'.

Tfrc, transferrin receptor protein 1; *Slc11a2*, solute carrier family 11 member 2; *Slc7a11*, solute carrier family seven member 11; *Gpx4*, glutathione peroxidase 4; *Ptgs2*, prostaglandin-endoperoxide synthase 2.

assessed (20). After treatment completion, the animals were anesthetized with 2% sodium pentobarbital (50 mg/kg) (B005, Jiancheng Bioengineering Institute) and sacrificed by cervical dislocation, and their hearts were removed. Myocardial tissues were fixed in 4% paraformaldehyde overnight at 4˚C, dehydrated in ascending ethanol gradient and embedded in paraffin for 2 h at room temperature and made into paraffin sections (5 μm). Subsequently, the sections were placed in an oven and heated at 60˚C for 1 h, immersed in xylene solution at room temperature for 10 min, and then immersed in descending ethanol gradient at room temperature for 5 min, followed by staining with hematoxylin and eosin at room temperature for 5 and 3 min, respectively, using an H&E staining kit (cat. no. C0105S; Beyotime Institute of Biotechnology). After dehydrating in 100% alcohol at room temperature for 5 min and mounting, tissues were observed under a microscope. Blood samples were taken from the abdominal aorta to detect brain natriuretic peptide (BNP) using a BNP ELISA Kit (cat. no. E-EL-R0126c; Elabscience Biotechnology, Inc.).

Statistical analysis. GraphPad Prism version 8.4.2 (GraphPad Software, Inc.) was used for statistical analysis. Data are presented as the mean ± standard deviation. Comparisons between two groups were performed using a Student's t-test, whereas an ANOVA followed by a Tukey's post hoc test was used to compare multiple groups. $P<0.05$ was considered to indicate a statistically significant difference.

Results

ECH ameliorates DOX-mediated increases in LDH and MDA levels and decreases in GSH levels in rat H9c2 cells. To determine the optimal concentration of ECH for regulating DOX-induced rat H9c2 cell cytotoxicity, H9c2 cells were cultured with ECH at various concentrations (5-20 μM) for 24 h, and the cell proliferation activity was detected using a CCK-8 assay kit (Fig. 1A). When 20 μM ECH was used, cell proliferation activity decreased significantly and in a dose-dependent manner. The MDA, GSH, and LDH levels were also measured. The MDA and LDH levels were elevated by DOX, whereas ECH significantly reduced this trend (Fig. 1B and C). Furthermore, when compared to the control group, the GSH levels in the DOX group were significantly lower, and an increase in this level was observed after ECH treatment (Fig. 1D).

ECH ameliorates DOX-induced ferroptosis in rat H9c2 cells. The mechanisms related to ferroptosis, such as iron homeostasis imbalance, GSH deficiency, oxidative stress, cardiac stimulation, and mitochondrial dysfunction, play a role in cardiac remodeling (14). Moreover, our previous study found that DOX caused cardiac injury by activating cardiomyocyte ferroptosis (7). Therefore, the effects of ECH on DOX-induced Fe^{2+} and lipid ROS in H9c2 cells were assessed. Interestingly, it was found that DOX exposure increased the Fe^{2+} levels in H9c2 cells by threefold when compared to the control group. However, ECH significantly reduced this elevation in a dose-dependent manner (from 5-20 μM; Fig. 2A). When H9c2 cells were treated with DOX, they produced significantly more lipid ROS as compared to the control group. Meanwhile, lipid ROS levels in the ECH groups were significantly reduced in a dose-dependent manner (Fig. 2B and C). GPX4 is currently recognized as a central inhibitor of ferroptosis, and its activity depends on glutathione produced by cystine-glutamate antitransporter solute carrier family seven member 11 (SLC7A11) activation, which is considered an anti-ferroptosis molecule (21). Additionally, transferrin receptor protein 1 (TFRC) is the key receptor mediating the cellular uptake of iron, and solute carrier family 11 member 2 (SLC11A2) is involved in the release of irons from acidified endosomes into the cytoplasm (22). Prostaglandin-endoperoxide synthase 2 (PTGS2) plays dual functions as both a cyclooxygenase and peroxidase, and is known to be induced by various ferroptosis inducers (22). Thus, the mRNA levels of hub ferroptosis-related genes *Tfrc*, *Slc11a2*, *Slc7a11*, *Gpx4*, and *Ptgs2* in cells were assessed. DOX exposure significantly increased the mRNA expression levels of *Tfrc*, *Slc11a2*, *Slc7a11*, and *Ptgs2*, while decreasing the mRNA expression levels of *Gpx4*. However, ECH significantly increased the mRNA expression levels of *Gpx4* and decreased the *Ptgs2* mRNA expression levels in DOX-treated rat H9c2 cells in a dose-dependent manner (Fig. 2D). These two proteins were therefore further examined by western blotting. DOX decreased GPX4 protein expression while increasing PTGS2 protein expression, and this was inhibited by ECH (Fig. 2E).

ECH inhibits erastin-induced ferroptosis in rat H9c2 cells. To further examine the role of ECH in ferroptosis in rat H9c2 cells, the ferroptosis inducer erastin was used. As illustrated in Fig. 3A, cell proliferation decreased significantly in erastin-treated cells, whereas ECH significantly increased

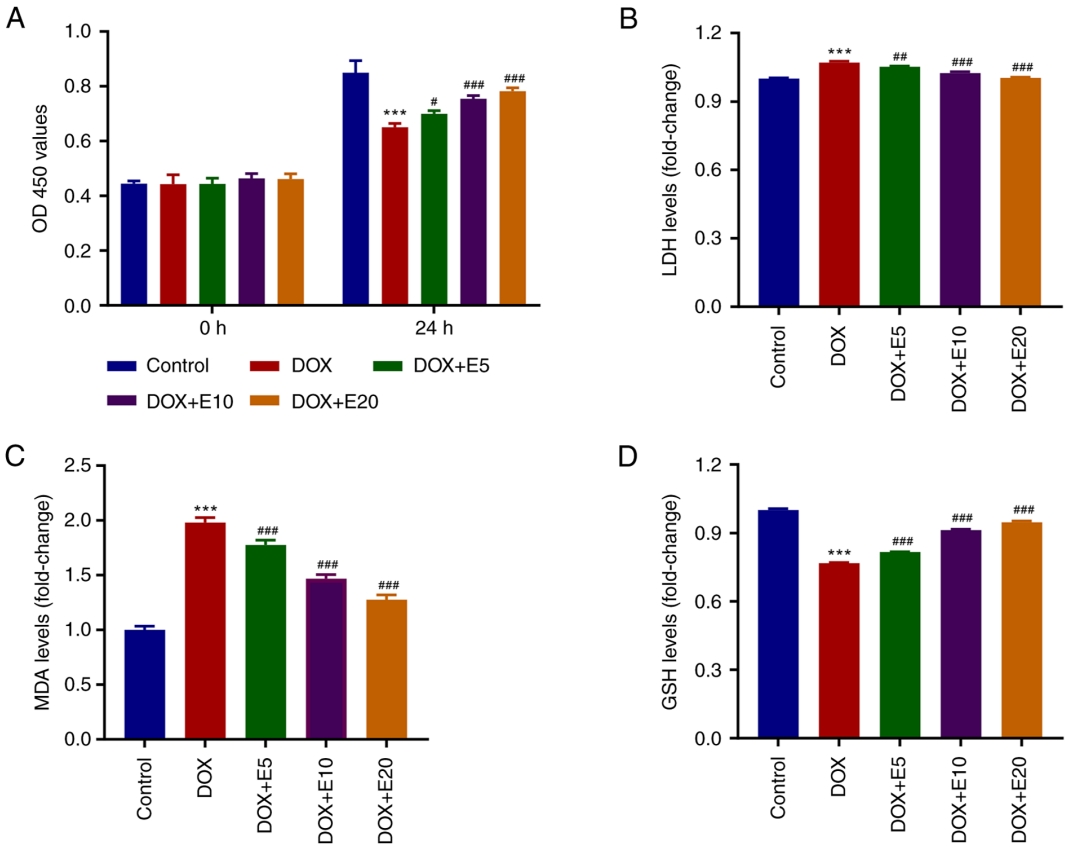

Figure 1. ECH ameliorates DOX-mediated increases in LDH and MDA levels and decreases in GSH levels in rat H9c2 cells. Rat H9c2 cells were treated with 2 μM DOX and 5, 10, or 20 μM ECH, and the (A) cell proliferation, (B) LDH, (C) MDA, and (D) GSH levels were measured. ***P<0.001 vs. control; $^{\#}$P<0.05, $^{\#\#}$P<0.01, $^{\#\#\#}$P<0.001 vs. DOX. ECH, Echinacoside; DOX, doxorubicin; LDH, lactate dehydrogenase; MDA, malondialdehyde; GSH, glutathione.

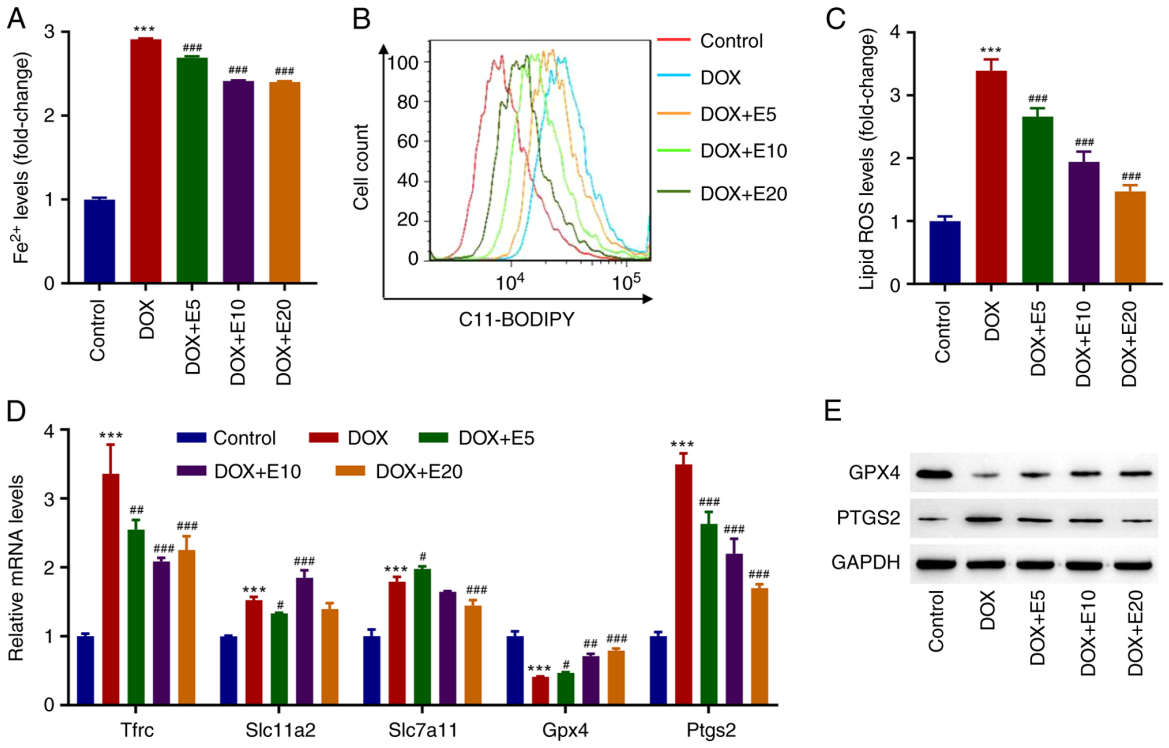

Figure 2. ECH reduced DOX-induced ferroptosis in rat H9c2 cells. Rat H9c2 cells were treated with 2 μM DOX and 5, 10, or 20 μM ECH, and the (A) Fe^{2+} concentrations, (B and C) lipid ROS levels, and (D) mRNA levels of *Tfrc*, *Slc11a2*, *Slc7a11*, *Gpx4* and *Ptgs2*, and (E) protein expression of GPX4 and PTGS2 were measured. ***P<0.001 vs. control; $^{\#}$P<0.05, $^{\#\#}$P<0.01, $^{\#\#\#}$P<0.001 vs. DOX. ECH, Echinacoside; DOX, doxorubicin; ROS, reactive oxygen species; *Tfrc*, transferrin receptor protein 1; *Slc11a2*, solute carrier family 11 member 2; *Slc7a11*, solute carrier family seven member 11; *Gpx4*, glutathione peroxidase 4; *Ptgs2*, prostaglandin-endoperoxide synthase 2.

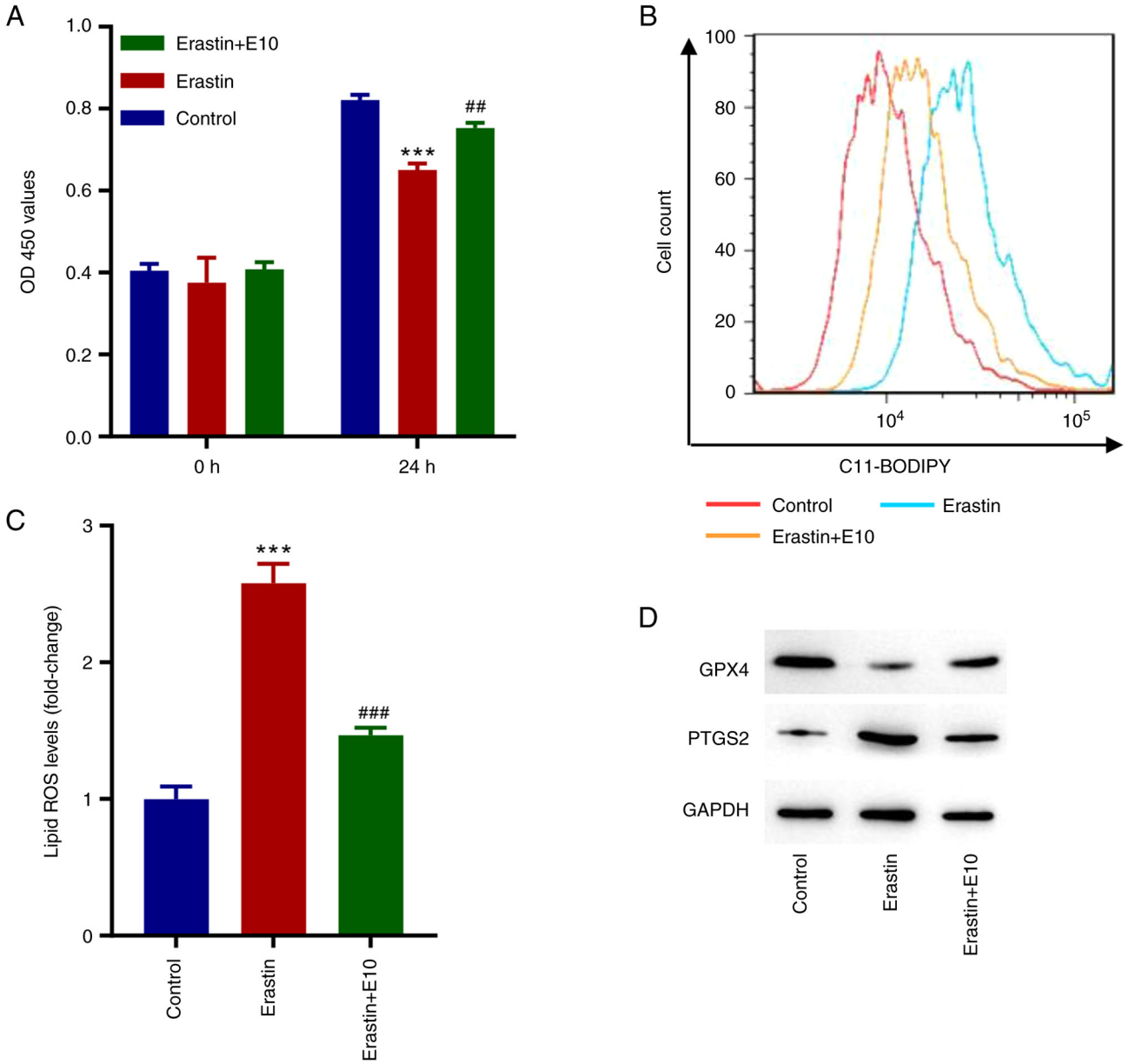

Figure 3. ECH prevents erastin-induced ferroptosis in rat H9c2 cells. Rat H9c2 cells were treated with 35 μM erastin and 10 μM ECH, and the (A) Fe^{2+} concentrations, (B and C) lipid ROS, and (D) protein expression levels of GPX4 and PTGS2 were measured. ***P<0.001 vs. control; $^{\#\#}$P<0.01, $^{\#\#\#}$P<0.001 vs. erastin. ECH, Echinacoside; ROS, reactive oxygen species; *Gpx4*, glutathione peroxidase 4; *Ptgs2*, prostaglandin-endoperoxide synthase 2.

cell proliferation after 24 h. Moreover, erastin significantly increased the lipid ROS levels, and ECH reversed this (Fig. 3B and C). When compared to the control group, erastin exposure reduced GPX4 expression while increasing PTGS2 expression, but ECH could reverse these effects (Fig. 3D).

Knockdown of Gpx4 inhibits the protective effects of ECH on DOX-induced accumulation of lipid ROS in rat H9c2 cells. shRNA targeting of *Gpx4* was used to investigate the effects of GPX4 on the protective effects of ECH on DOX-induced ferroptosis in rat H9c2 cells. Western blot analysis revealed that using specific *Gpx4* shRNAs (Fig. 4A and B) significantly reduced *Gpx4* expression when compared to the shNC group. Furthermore, ECH significantly reduced the DOX-induced increases in lipid ROS levels, whereas shGpx4 reversed this effect (Fig. 4C and D). Additionally, Western blotting data showed that DOX inhibited GPX4 expression while increasing PTGS2 expression; however, this trend was reversed by the knockdown of *Gpx4* (Fig. 4E). These findings showed that knockdown of *Gpx4* inhibited the protective effects of ECH on DOX-induced accumulation of lipid ROS in rat H9c2 cells.

ECH ameliorates DOX-induced CHF in rats. DOX was used to establish a CHF rat model to assess the effects of ECH on CHF *in vivo*. DOX reduced the left ventricular ejection fraction, fractional shortening, end-systolic pressure, and heart rate while increasing left ventricular end-diastolic pressure (Table II). Conversely, ECH may improve DOX-induced cardiac function. Tissue sections from the control group exhibited a normal morphology, whereas those from DOX-treated rats exhibited myocardial disorganization, increased intracellular spaces, and cytoplasmic vacuolization (Fig. 5A).

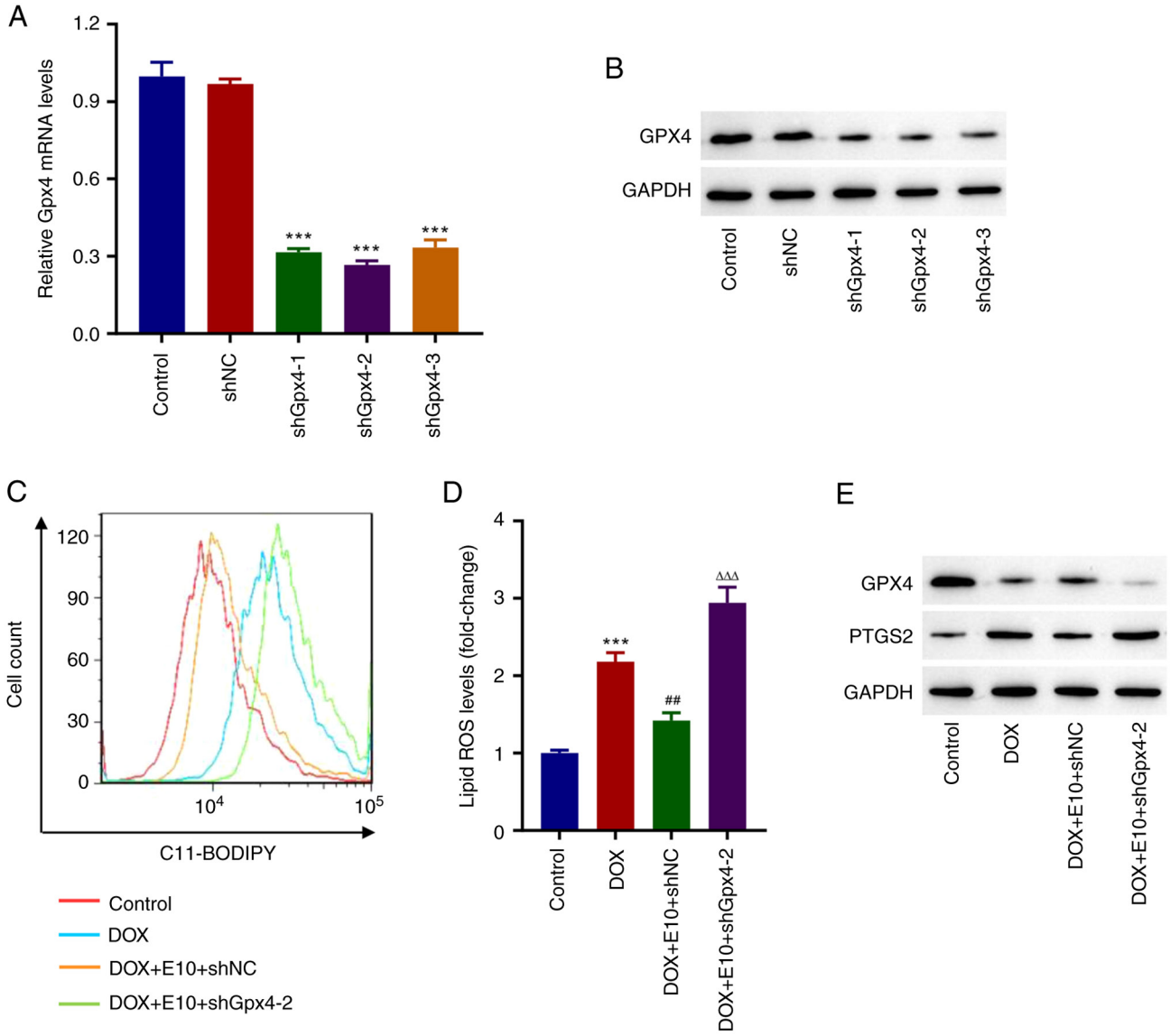

Figure 4. *Gpx4* knockdown inhibits the protective effects of ECH on DOX-induced accumulation of lipid ROS in rat H9c2 cells. (A) *Gpx4* mRNA and (B) protein expression levels in rat H9c2 cells transduced with lentiviral plasmids containing *Gpx4* shRNA. Rat H9c2 cells transduced with lentiviral plasmid expressing *Gpx4* shRNA were treated with 2 μM DOX and 10 μM ECH, and the (C and D) lipid ROS and (E) protein expression levels of GPX4 and PTGS2 were measured. ***P<0.001 vs. control; $^{\#\#}$P<0.01 vs. DOX; $^{\Delta\Delta\Delta}$P<0.001 vs. DOX + E10 + shNC. ECH, Echinacoside; DOX, doxorubicin; Gpx4, glutathione peroxidase 4; ROS, reactive oxygen species; shRNA, short hairpin; PTGS2, prostaglandin-endoperoxide synthase 2; NC, negative control.

Moreover, eosinophilic cells with pyknotic nuclei and loss of myofibrils were observed among cardiomyocytes in the DOX-treated rats (Fig. 5A). However, ECH administration resulted in a considerable improvement in the histopathology as compared to that observed in the DOX group; the histological appearance of high-dose ECH group was similar to that of the control group (Fig. 5A). Given that BNP is an important indicator of ventricular function, the BNP levels in the CHF rat model were measured by ELISA. The findings revealed that, when compared to the control group, DOX exposure significantly increased the BNP levels, whereas ECH exposure decreased the BNP levels in a dose-dependent manner (Fig. 5B). LDH is an enzyme found in myocardial cell damage. DOX significantly increased the LDH levels compared with the control group, whereas ECH administration reversed this effect (Fig. 5C). Of note, the effect of ECH on the protein expression levels of GPX4 and PTGS2 matched the *in vitro* findings, which showed that ECH administration reversed the effects in the CHF rat model (Fig. 5D).

Discussion

HF is a complicated clinical syndrome characterized by cardiac systolic and diastolic dysfunction (23). Despite numerous clinical and experimental studies on the treatment of CHF, a satisfactory treatment regimen to prevent HF progression is lacking (24). Hence, it is critical to find a safe and effective therapeutic to treat HF. ECH has been studied for its potential to protect against HF (25). The effect and molecular mechanism of HF, however, are unknown.

In the present study, ECH protected DOX-treated H9c2 cells from oxidative stress and ferroptosis. Furthermore, ECH alleviated DOX-induced cardiac injury by regulating GPX4 inhibition-induced ferroptosis. A growing body of evidence

Table II. Cardiac parameters in the rat models of heart failure.

Group	Echocardiographic data, %		Left ventricular end pressure, mmHg		Heart rate, beats/min
	Ejection fraction	Fractional shortening	Systolic	Diastolic	
Control	85.33±1.72	47.33±2.08	102.89±0.59	7.53±0.78	370.00±9.42
DOX	60.54±4.45[a]	26.74±2.78[a]	71.98±1.54[a]	12.57±0.21[a]	298.17±9.15[a]
DOX+E50	73.25±3.37[c]	35.66±2.67[c]	79.31±1.75[c]	11.78±0.56[b]	308.17±11.05
DOX+E100	83.17±1.45[c]	44.83±1.64[c]	94.63±6.19[c]	10.72±0.40[c]	338.00±5.83[c]

[a]P<0.05, [b]P<0.01, [c]P<0.001 vs. DOX. ECH, Echinacoside; E50, 50 mg/kg ECH; E100, 100 mg/kg ECH; DOX, doxorubicin. Data are presented as the mean ± standard deviation.

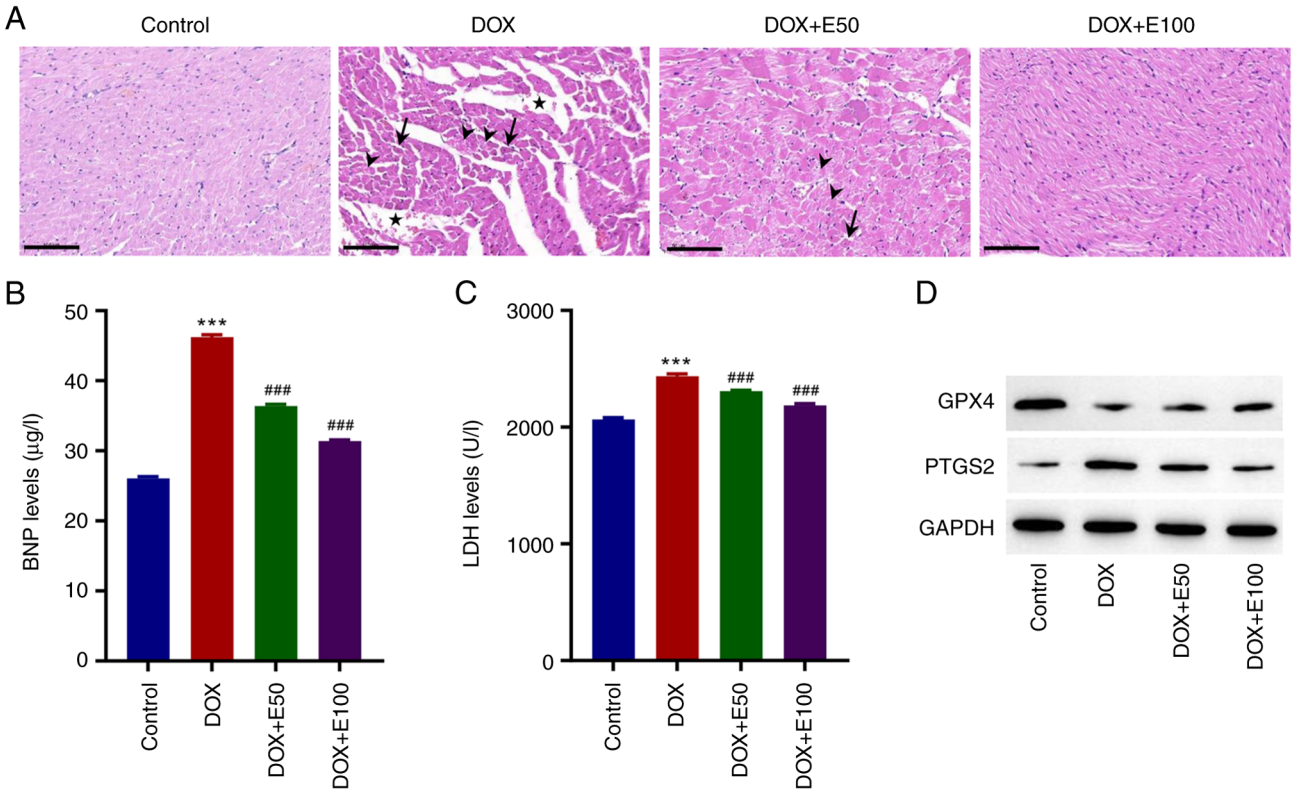

Figure 5. ECH reduced the DOX-induced cardiac injury in rat. (A) Images of hematoxylin and eosin-stained cardiomyocytes. Scale bar, 100 μm. Serum (B) BNP and (C) LDH levels. (D) Protein expression levels of GPX4 and PTGS2. Stars, intracellular spaces; arrowheads, myofibril loss; black arrows, eosinophilia and pyknotic nuclei. ***P<0.001 vs. control; ###P<0.001 vs. DOX. ECH, Echinacoside; DOX, doxorubicin; *Gpx4*, glutathione peroxidase 4; PTGS2, prostaglandin-endoperoxide synthase 2; BNP, brain natriuretic peptide; LDH, lactate dehydrogenase.

suggests that oxidative stress is a direct or indirect pathophysiological pathway in the HF process (26). Excess ROS production causes cellular protein, lipid, and DNA damage, and the physiological antioxidant defense system cannot eliminate it, resulting in cell necrosis and apoptosis (27). MDA is formed as the result of lipid oxidation by oxygen-free radicals, causing cytotoxicity and worsening cell membrane damage, and is commonly used to reflect the degree of oxidative stress (28,29). However, an excess of ROS leads to an excess of lipid peroxide conversion in HF development. Meanwhile, MDA production increases, activating a feedforward loop mechanism, and oxidative stress increases, resulting in further deterioration of myocardial systolic and diastolic functions (30). DOX was found to increase the production of inflammatory cytokines during cardiotoxicity and oxidative stress (31,32). When patients develop HF, the plasma BNP levels are markedly increased, and the degree of increase is related to the degree of ventricular dilatation, which is widely used as an HF biomarker, and is involved in ventricular dysfunction; that is, the content of BNP is closely associated with HF severity (33,34). In the present study, the effects of ECH on DOX-induced BNP in plasma for the alleviation of HF symptoms were investigated. The results showed that ECH effectively alleviated cardiac injury *in vivo* and *in vitro*.

As more evidence emerged that myocardial cell ferroptosis is associated with myocardial ischemia-reperfusion injury, which plays a role in HF development, it was shown that ferroptosis inhibition could improve myocardial injury and HF (35-38). Ferroptosis is caused by an imbalance in the production and clearance of intracellular lipid peroxides (39). Ferroptosis involves lipid, GSH, and iron metabolisms, and mitochondrial dysfunction. When cells experience iron overload, the ROS levels increase, resulting in intracellular lipid peroxide accumulation, and iron overload in cardiomyocytes results in oxidative stress and mitochondrial damage, eventually leading to systolic and diastolic dysfunction and myocardial fibrosis (40,41). Iron overload damages the heart by causing oxidative stress, promoting HF development (42). According to research, inhibiting GSH synthesis increases cardiac lipid peroxidation, which inhibits myocardial contractility (43). One of the ferroptosis-related proteins is GPX4, and selenium deficiency is a risk factor for HF development. By lowering the GPX4 activity, selenium deficiency promotes CHF progression. PTGS2 participated in the prostaglandin biosynthesis process, which catalyzes lipid oxidation and is involved in ferroptosis (44). Furthermore, it was discovered that ECH administration decreased PTGS2 expression while increasing GPX4 expression in DOX-treated rats and H9c2 cells. As a regulator of ferroptosis, GPX4 induces ferroptosis by inhibiting its substrate glutathione or glutathione components (45). When cardiomyocytes produce a large amount of ROS, the cell's antioxidant activity is reduced, and lipid ROS are produced, inhibiting GSH absorption, and the GSH levels are associated with HF severity (46). GSH deficiency causes cysteine deficiency, lowering the GPX4 activity and resulting in ferroptosis. Furthermore, *Gpx4* knockdown inhibited the protective effects of ECH on DOX-induced accumulation of lipid ROS in rat H9c2 cells, indicating that ECH could protect DOX-induced cardiac injury by affecting ferroptosis hub proteins. These important findings provide a foundation for the clinical treatment of CHF. Owing to the limited literature reports on the involvement of ferroptosis in CHF, the present study may be considered for developing a potential therapy for the disease based on targeting of ferroptosis.

In conclusion, ECH ameliorated DOX-induced cardiac injury by regulating GPX4 inhibition-induced ferroptosis. Thus, ECH may serve as a promising and important therapy for the treatment of CHF injury.

Acknowledgements

Not applicable.

Funding

The present study was financially supported by the Shanghai Pudong Commission of Health and Family Planning (grant no. PW2020D-10), Shanghai Municipal Commission of Health and Family Planning (grant no. 202040188), Medical Disciplinary Development Project of Pudong New Area Health System (grant no. PWYgy2021-10) and Multiplication plan for traditional Chinese medicine specialty brand building (grant no. PDZY-2021-0310).

Availability of data and material

The datasets used and/or analyzed during the present study are available from the corresponding author on reasonable request.

Authors' contributions

YM, SZ, and JZ conceived and designed the study. YM wrote, reviewed, and revised the manuscript. XY, NJ, CL and JZ acquired, analyzed, and interpreted the data, and performed the statistical analysis. YM, SZ, and JZ confirm the authenticity of all the raw data. All authors have read and approved the final manuscript.

Ethics approval and consent to participate

All experimental procedures were performed in accordance with the Guidelines for the Institutional Animal Care and Use Committee of Shanghai Rat & Mouse Biotech Co., Ltd. (approval no. 202109).

Patient consent for publication

Not applicable.

Competing interests

The authors declare that they have no competing interests.

References

1. Sola S, Mir MQS, Lerakis S, Tandon N and Khan BV: Atorvastatin improves left ventricular systolic function and serum markers of inflammation in nonischemic heart failure. J Am Coll Cardiol 47: 332-337, 2006.
2. Wen W, Zhang Z, She J, Bai X, Wu Y, Gao L, Zhou J and Yuan Z: The predictive values of white blood cell indices (lymphocyte and eosinophilic granulocyte) for heart failure in acute coronary syndrome patients following percutaneous coronary intervention: A prospective cohort study. Clin Interv Aging 18: 951-962, 2023.
3. Khan H, Anker SD, Januzzi JL Jr, McGuire DK, Sattar N, Woerle HJ and Butler J: Heart failure epidemiology in patients with diabetes mellitus without coronary heart disease. J Card Fail 25: 78-86, 2019.
4. Hunt SA, Abraham WT, Chin MH, Feldman AM, Francis GS, Ganiats TG, Jessup M, Konstam MA, Mancini DM, Michl K, *et al*: ACC/AHA 2005 guideline update for the diagnosis and management of chronic heart failure in the adult: A report of the American college of cardiology/American heart association task force on practice guidelines (writing committee to update the 2001 guidelines for the evaluation and management of heart failure): Developed in collaboration with the American college of chest physicians and the international society for heart and lung transplantation: Endorsed by the heart rhythm society. Circulation 112: e154-e235, 2005.
5. Long K, Zhao Z, Chen J, Zhi L, Wang C, Liao D, Wang M and Gao P: Yang-xin-xue keli exerts therapeutic effects via regulating mitochondrial homeostasis and function in doxorubicin-induced rat heart failure. Front Pharmacol 13: 931453, 2022.
6. Ermis N, Ulutas Z, Ozhan O, Yildiz A, Vardi N, Colak C and Parlakpinar H: Angiotensin II type 2 receptor agonist treatment of doxorubicin induced heart failure. Biotech Histochem 98: 326-335, 2023.
7. Zhuang S, Ma Y, Zeng Y, Lu C, Yang F, Jiang N, Ge J, Ju H, Zhong C, Wang J, *et al*: METTL14 promotes doxorubicin-induced cardiomyocyte ferroptosis by regulating the KCNQ1OT1-miR-7-5p-TFRC axis. Cell Biol Toxicol 39: 1015-1035, 2023.

8. Liao HH, Ding W, Zhang N, Zhou ZY, Ling Z, Li WJ, Chen S and Tang QZ: Activation of AMPKα2 attenuated doxorubicin-induced cardiotoxicity via inhibiting lipid peroxidation associated ferroptosis. Free Radic Biol Med 205: 275-290, 2023.
9. Syamprasad NP, Jain S, Rajdev B, Panda SR, Gangasani JK, Challa VS, Vaidya JR, Kundu GC and Naidu VGM: AKR1B1 inhibition using NARI-29-an epalrestat analogue-alleviates doxorubicin-induced cardiotoxicity via modulating calcium/CaMKII/MuRF-1 axis. Chem Biol Interact 381: 110566, 2023.
10. Yang J, Ma S, Xu R, Wei Y, Zhang J, Zuo T, Wang Z, Deng H, Yang N and Shen Q: Smart biomimetic metal organic frameworks based on ROS-ferroptosis-glycolysis regulation for enhanced tumor chemo-immunotherapy. J Control Release 334: 21-33, 2021.
11. Wang R, Chen X, Li X and Wang K: Molecular therapy of cardiac ischemia-reperfusion injury based on mitochondria and ferroptosis. J Mol Med (Berl): Jul 28, 2023 (Epub ahead of print).
12. Kumarswamy R and Thum T: Non-coding RNAs in cardiac remodeling and heart failure. Circ Res 113: 676-689, 2013.
13. Matsumoto T, Wada A, Tsutamoto T, Ohnishi M, Isono T and Kinoshita M: Chymase inhibition prevents cardiac fibrosis and improves diastolic dysfunction in the progression of heart failure. Circulation 107: 2555-2558, 2003.
14. Zy A, Gd A, Xu CA, Qin X, Xu H, Zeng B, Ren J, Zheng Q and Wang S: Beclin1 haploinsufficiency rescues low ambient temperature-induced cardiac remodeling and contractile dysfunction through inhibition of ferroptosis and mitochondrial injury. Metabolism 113: 154397, 2020.
15. Chen X, Xu S, Zhao C and Liu B: Role of TLR4/NADPH oxidase 4 pathway in promoting cell death through autophagy and ferroptosis during heart failure. Biochem Biophys Res Commun 516: 37-43, 2019.
16. Zhang H, Zhabyeyev P, Wang S and Oudit GY: Role of iron metabolism in heart failure: From iron deficiency to iron overload. Biochim Biophys Acta Mol Basis Dis 1865: 1925-1937, 2019.
17. Zhang D, Li H and Wang JB: Echinacoside inhibits amyloid fibrillization of HEWL and protects against Aβ-induced neurotoxicity. Int J Biol Macromol 72: 243-253, 2015.
18. Yang X, Li F, Yang Y, Shen J, Zou R, Zhu P, Zhang C, Yang Z and Li P: Efficacy and safety of echinacoside in a rat osteopenia model. Evid Based Complement Alternat Med 2013: 926928, 2013.
19. Livak KJ and Schmittgen TD: Analysis of relative gene expression data using real-time quantitative PCR and the 2(-Delta Delta C(T)) method. Methods 25: 402-408, 2001.
20. Yao L, Gui M, Li J, Lu B, Wang J, Zhou X and Fu D: Shengxian decoction decreases doxorubicin-induced cardiac apoptosis by regulating the TREM1/NF-κB signaling pathway. Mol Med Rep 23: 219, 2021.
21. Chen H, Wang L, Liu J, Wan Z, Zhou L, Liao H and Wan R: LncRNA ITGB2-AS1 promotes cisplatin resistance of non-small cell lung cancer by inhibiting ferroptosis via activating the FOSL2/NAMPT axis. Cancer Biol Ther 24: 2223377, 2023.
22. Yuan H, Xia P, Sun X, Ma J, Xu X, Fu C, Zhou H, Guan Y, Li Z, Zhao S, *et al*: Photothermal nanozymatic nanoparticles induce ferroptosis and apoptosis through tumor microenvironment manipulation for cancer therapy. Small 18: e2202161, 2022.
23. Aurigemma GP, Gottdiener JS, Shemanski L, Gardin J and Kitzman D: Predictive value of systolic and diastolic function for incident congestive heart failure in the elderly: The cardiovascular health study. J Am Coll Cardiol 37: 1042-1048, 2001.
24. Bonsu KO, Owusu IK, Buabeng KO, Reidpath DD and Kadirvelu A: Review of novel therapeutic targets for improving heart failure treatment based on experimental and clinical studies. Ther Clin Risk Manag 12: 887-906, 2016.
25. Ni Y, Zhang J, Zhu W, Duan Y, Bai H and Luan C: Echinacoside inhibited cardiomyocyte pyroptosis and improved heart function of HF rats induced by isoproterenol via suppressing NADPH/ROS/ER stress. J Cell Mol Med 26: 5414-5425, 2022.
26. Landmesser U, Spiekermann S, Dikalov S, Tatge H, Wilke R, Kohler C, Harrison DG, Hornig B and Drexler H: Vascular oxidative stress and endothelial dysfunction in patients with chronic heart failure: Role of xanthine-oxidase and extracellular superoxide dismutase. Circulation 106: 3073-3078, 2002.
27. Xiang XY, Yang XC, Su J, Kang JS, Wu Y, Xue YN, Dong YT and Sun LK: Inhibition of autophagic flux by ROS promotes apoptosis during DTT-induced ER/oxidative stress in HeLa cells. Oncol Rep 35: 3471-3479, 2016.
28. Ergüç A, Karakuş F, Arzuk E, Mutlu N and Orhan H: Role of oxidative stress and reactive metabolites in cytotoxicity & mitotoxicity of clozapine, diclofenac and nifedipine in CHO-K1 cells in vitro. Endocr Metab Immune Disord Drug Targets: Apr 19, 2023 (Epub ahead of print).
29. Granieri MC, Rocca C, De Bartolo A, Nettore IC, Rago V, Romeo N, Ceramella J, Mariconda A, Macchia PE, Ungaro P, *et al*: Quercetin and its derivative counteract palmitate-dependent lipotoxicity by inhibiting oxidative stress and inflammation in cardiomyocytes. Int J Environ Res Public Health 20: 3492, 2023.
30. Turk R, Juretić D, Geres D, Svetina A, Turk N and Flegar-Mestrić Z: Influence of oxidative stress and metabolic adaptation on PON1 activity and MDA level in transition dairy cows. Anim Reprod Sci 108: 98-106, 2008.
31. Ichihara S, Yamada Y, Kawai Y, Osawa T, Furuhashi K, Duan Z and Ichihara G: Roles of oxidative stress and Akt signaling in doxorubicin cardiotoxicity. Biochem Biophys Res Commun 359: 27-33, 2007.
32. Birari L, Wagh S, Patil KR, Mahajan UB, Unger B, Belemkar S, Goyal SN, Ojha S and Patil CR: Aloin alleviates doxorubicin-induced cardiotoxicity in rats by abrogating oxidative stress and pro-inflammatory cytokines. Cancer Chemother Pharmacol 86: 419-426, 2020.
33. Gaggin HK and Januzzi JL Jr: Biomarkers and diagnostics in heart failure. Biochim Biophys Acta 1832: 2442-2450, 2013.
34. Salah K, Stienen S, Pinto YM, Eurlings LW, Metra M, Bayes-Genis A, Verdiani V, Tijssen JGP and Kok WE: Prognosis and NT-proBNP in heart failure patients with preserved versus reduced ejection fraction. Heart 105: 1182-1189, 2019.
35. Liu B, Zhao C, Li H, Chen X, Ding Y and Xu S: Puerarin protects against heart failure induced by pressure overload through mitigation of ferroptosis. Biochem Biophys Res Commun 497: 233-240, 2018.
36. Conrad M and Proneth B: Broken hearts: Iron overload, ferroptosis and cardiomyopathy. Cell Res 29: 263-264, 2019.
37. Fang X, Cai Z, Wang H, Han D, Cheng Q, Zhang P, Gao F, Yu Y, Song Z, Wu Q, *et al*: Loss of cardiac ferritin H facilitates cardiomyopathy via Slc7a11-mediated ferroptosis. Circ Res 127: 486-501, 2020.
38. Fang X, Wang H, Han D, Xie E, Yang X, Wei J, Gu S, Gao F, Zhu N, Yin X, *et al*: Ferroptosis as a target for protection against cardiomyopathy. Proc Natl Acad Sci USA 116: 2672-2680, 2019.
39. Miess H, Dankworth B, Gouw AM, Rosenfeldt M, Schmitz W, Jiang M, Saunders B, Howell M, Downward J, Felsher DW, *et al*: The glutathione redox system is essential to prevent ferroptosis caused by impaired lipid metabolism in clear cell renal cell carcinoma. Oncogene 37: 5435-5450, 2018.
40. Wu T, Liang X, Liu X, Li Y, Wang Y, Kong L and Tang M: Induction of ferroptosis in response to graphene quantum dots through mitochondrial oxidative stress in microglia. Part Fibre Toxicol 17: 30, 2020.
41. Paterek A, Mackiewicz U and Mączewski M: Iron and the heart: A paradigm shift from systemic to cardiomyocyte abnormalities. J Cell Physiol 234: 21613-21629, 2019.
42. Cheng CF and Lian WS: Prooxidant mechanisms in iron overload cardiomyopathy. Biomed Res Int 2013: 740573, 2013.
43. Chen L, Yin Z, Qin X, Zhu X, Chen X, Ding G, Sun D, Wu NN, Fei J, Bi Y, et al: CD74 ablation rescues type 2 diabetes mellitus-induced cardiac remodeling and contractile dysfunction through pyroptosis-evoked regulation of ferroptosis. Pharmacol Res 176, 2022.
44. Yang WS, SriRamaratnam R, Welsch ME, Shimada K, Skouta R, Viswanathan VS, Cheah JH, Clemons PA, Shamji AF, Clish CB, *et al*: Regulation of ferroptotic cancer cell death by GPX4. Cell 156: 317-331, 2014.
45. Wu J, Minikes AM, Gao M, Bian H, Li Y, Stockwell BR, Chen ZN and Jiang X: Intercellular interaction dictates cancer cell ferroptosis via NF2-YAP signalling. Nature 572: 402-406, 2019.
46. Ren J, Privratsky JR, Yang X, Dong F and Carlson EC: Metallothionein alleviates glutathione depletion-induced oxidative cardiomyopathy in murine hearts. Crit Care Med 36: 2106-2116, 2008.